JOURNAL OF VIROLOGY, Nov. 1995, p. 7072–7086 Vol. 69, No. 11
0022-538X/95/$04.00+0

Characterization of *ts*16, a Temperature-Sensitive Mutant of Vaccinia Virus

MARIA ERICSSON,[1] SALLY CUDMORE,[1] STEWART SHUMAN,[2] RICHARD C. CONDIT,[3] GARETH GRIFFITHS,[1]* AND JACOMINE KRIJNSE LOCKER[1]

Cell Biology Programme, European Molecular Biology Laboratory, 69012 Heidelberg, Germany[1]; Program in Molecular Biology, Sloan-Kettering Institute, New York, New York 10021[2]; and Department of Immunology and Medical Microbiology, University of Florida, Gainesville, Florida 32610-0266[3]

Received 15 May 1995/Accepted 8 August 1995

We have characterized a temperature-sensitive mutant of vaccinia virus, *ts*16, originally isolated by Condit et al. (Virology 128:429–443, 1983), at the permissive and nonpermissive temperatures. In a previous study by Kane and Shuman (J. Virol 67:2689–2698, 1993), the mutation of *ts*16 was mapped to the I7 gene, encoding a 47-kDa protein that shows partial homology to the type II topoisomerase of *Saccharomyces cerevisiae*. The present study extends previous electron microscopy analysis, showing that in BSC40 cells infected with *ts*16 at the restrictive temperature (40°C), the assembly was arrested at a stage between the spherical immature virus and the intracellular mature virus (IMV). In thawed cryosections, a number of the major proteins normally found in the IMV were subsequently localized to these mutant particles. By using sucrose density gradients, the *ts*16 particles were purified from cells infected at the permissive and nonpermissive temperatures. These were analyzed by immunogold labelling and negative-staining electron microscopy, and their protein composition was determined by sodium dodecyl sulfate-polyacrylamide gel electrophoresis. While the *ts*16 virus particles made at the permissive temperature appeared to have a protein pattern identical to that of wild-type IMV, in the mutant particles the three core proteins, p4a, p4b, and 28K, were not proteolytically processed. Consistent with previous data the sucrose-purified particles could be labelled with [^{3}H]thymidine. In addition, anti-DNA labelling on thawed cryosections suggested that most of the mutant particles had taken up DNA. On thawed cryosections of cells infected at the permissive temperature, antibodies to I7 labelled the virus factories, the immature viruses, and the IMVs, while under restrictive conditions these structures were labelled much less, if at all. Surprisingly, however, by Western blotting (immunoblotting) the I7 protein was present in similar amounts in the defective particles and in the IMVs isolated at the permissive temperature. Finally, our data suggest that at the nonpermissive temperature the assembly of *ts*16 is irreversibly arrested in a stage at which the DNA is in the process of entering but before the particle has completely sealed, as monitored by protease experiments.

Vaccinia virus (VV) morphogenesis has been extensively studied by electron microscopy (EM) and biochemistry (for reviews, see references 6, 11, 19, and 25). Viral DNA replication and assembly occur in the cytoplasms of infected cells, in discrete structures referred to as viral factories (2, 5, 20). The first characteristic viral structures to appear during assembly are crescent-shaped membranes (5, 7). We have recently shown that these crescents consist of two membranes that are continuous with the membrane of the intermediate compartment between the endoplasmic reticulum (ER) and the Golgi complex (43). The crescents mature into spherical immature virions (IVs), which are not sealed and which have not yet taken up the viral DNA. These IVs then undergo a complex series of maturational events, including uptake of the genome and proteolytical processing of viral core proteins (26, 40, 47, 49). The product of these events is the first infectious form of the virus, which we have proposed be called the intracellular mature virus (IMV) (43). In most cell types a variable fraction of the IMVs become further engulfed by a cisterna that originates from the trans-Golgi network, thereby forming the precursor of the second infectious form of the virus, the extracellular enveloped virus (14, 29, 39).

* Corresponding author. Mailing address: Cell Biology Programme, European Molecular Biology Laboratory, Postfach 10.2209, 69012 Heidelberg, Germany.

During the transition from the IV to the IMV, an intermediate structure can be seen by electron microscopy (13). This intermediate appears to be more condensed than the IV and can be characterized by the acquisition of p14, a peripheral membrane protein found also on the outside of the IMV (42). The transition from the IV to the IMV is further associated with a complex and poorly understood process by which the DNA enters the viral particle (5, 13, 24). Our understanding of the molecular mechanisms involved in the formation of the IMV lags significantly behind the descriptive morphological data. A serious obstacle in following the molecular events has been the difficulty in isolating intermediate stages. Whereas the IMV can be purified by using either sucrose or cesium chloride gradients (8), reports on the isolation of earlier stages of the assembly process have been sparse (36).

In the present study we have used a temperature-sensitive mutant of VV, *ts*16. This mutant VV was first described by Condit et al. (4) and was classified as having normal DNA and protein synthesis. More recently the mutation of *ts*16 has been mapped to a single amino acid substitution (Pro to Leu at position 344) in the product of the I7 gene (21). This gene encodes a 47-kDa late protein that has approximately 20% homology over a stretch of 200 amino acids to the *Saccharomyces cerevisiae* type II DNA topoisomerase. By EM it was shown that at the restrictive temperature of 40°C the assembly was arrested at a stage intermediate between the IV and the

IMV, a stage at which the DNA entry occurs. The mutant protein appeared to be made normally at 40°C, but it was not assessed whether it was present in the viral particles that accumulate at the nonpermissive temperature (21). In wild-type VV the I7 protein was associated with the viral core fraction, as analyzed biochemically (21). In this study we have further characterized the *ts*16 mutant using both morphological and biochemical approaches and have developed a procedure to purify the intermediate particle that was arrested at the nonpermissive temperature.

MATERIALS AND METHODS

Cells and viruses. BSC40 cells were grown in Dulbecco's modified Eagle's medium (DMEM) supplemented with 5% heat-inactivated fetal calf serum. HeLa cells were grown in Eagle's minimal essential medium supplemented with 10% heat-inactivated fetal calf serum and nonessential amino acids. The wild-type VV strain WR was propagated in HeLa cells grown at 37°C as previously described (9). VV *ts*16 was amplified in BSC40 cells at 31°C (permissive temperature).

Antibodies. The antibody recognizing p25 (L4R) was a kind gift from D. Hruby (48). The peptide antibody recognizing the COOH terminus of p4a (A10L) was a kind gift from R. Doms and was made by using the peptide MTDGDSVSFDDE. This peptide was coupled to keyhole limpet hemocyanin and used for three immunizations of rabbits, one primary immunization followed by two boosters at 4-week intervals. The anti-I7 antibody has been described earlier (21). The anti-DNA monoclonal antibody was purchased from Boehringer (Mannheim, Germany). The following antibodies were provided from the indicated sources: anti-p32 (D8L gene) antiserum (D8.1) from G. Niles (28), anti-p14 (A27L gene) monoclonal antibody (C3) from M. Esteban (32), anti-p4a/4a recognizing the precursor (p4a) and processed form of 4a (3160) (49), anti-p4b/4b and anti-p28/p25 (48) from D. Hruby, and the peptide antibody (B1) against the COOH terminus of p65 (D13L) from R. W. Doms (44).

EM. Confluent BSC40 cells were infected with VV *ts*16 virus in phosphate-buffered saline (PBS) (with Mg^{2+} and Ca^{2+}) at a multiplicity of infection of 10 at 31 and 40°C. After a 1-hour adsorption, the inoculum was aspirated, and the cells were washed once with PBS and then overlaid with DMEM which had been prewarmed to the appropriate temperature. At various times after infection, cells were processed for Epon embedding and postembedding immunolabelling as follows. For Epon embedding, cells were fixed on the dish for 60 min in 1% glutaraldehyde in 200 mM cacodylate buffer (pH 7.4), stained with a mixture of 2% OsO_4 and 1.5% KFe CN_6 for 1 h and with 1% magnesium uranyl acetate for 30 min, and then processed for conventional Epon embedding (12). For preparation of cryosections, infected cells were removed from the dish with proteinase K (25 μg/ml) on ice and then centrifuged at 800 × *g* for 3 min, and the pellet was fixed overnight with 8% paraformaldehyde in 250 mM HEPES (*N*-2-hydroxyethylpiperazine-*N*′-2-ethanesulfonic acid), pH 7.4. Prior to freezing in liquid nitrogen the cell pellets were infiltrated with 2.1 M sucrose in PBS for 15 min. Frozen samples were sectioned at −90°C, the sections were transferred to Formvar-coated copper grids, and immunolabelling was carried out as described elsewhere (12). The procedure for negative staining with ammonium molybdate-methylcellulose is also given in reference 12.

Visualization of isolated virus particles was performed by negative staining with 2% ammonium molybdate. To immunolabel the isolated virus particles, a drop of material was adsorbed to a copper grid for 5 min, and the grid was washed briefly in PBS and then incubated on a drop of antibody for 15 min. Following rinses on 4 drops of PBS for a total of 10 min the grid was incubated with protein A-gold for 15 min. A final 15-min wash on 4 drops of PBS was followed by a brief rinse in water before negative staining with ammonium molybdate for 1 min.

Proteinase K and DNase treatment of *ts*16-infected cells. BSC40 cells infected with *ts*16 for 24 h at 40°C were put on ice and rinsed twice in ice-cold streptolysin O (SLO) buffer (150 mM sucrose, 25 mM HEPES [pH 7.4], 115 mM potassium acetate, 2.5 mM $MgCl_2$). Cells were incubated with 2 U of SLO (Wellcome Diagnostics) per ml for 10 min on ice. To remove unbound SLO, the cells were washed in SLO buffer containing 1 mM freshly made dithiothreitol (DTT; Boehringer GmbH) and then permeabilized in this buffer by a 20-min incubation at 40°C. Cells were put on ice again, washed twice in SLO buffer, and overlaid with SLO buffer containing 1 mg of proteinase K per ml. For the treatment with DNase, the permeabilized cells were incubated for 30 min at 37°C in SLO buffer containing 500 U of DNase I (Sigma) per ml. In some experiments the permeabilized cells were incubated with distilled water for 10 min. The cells detached by themselves from the dish in the proteinase K solution or were scraped and transferred to an Eppendorf tube and incubated at 4°C on a rocking table. After 60 min cells were spun for 2 min at 2,000 × *g*, and the pellet was fixed with 1% glutaraldehyde in 200 mM HEPES (pH 7.4) for 30 min at room temperature. Cell pellets were processed for either Epon embedding or cryosectioning as described above.

Metabolic labelling. BSC40 cells in 35-mm-diameter dishes were infected as described above. After 1 h the cells were washed once in ice-cold PBS and then overlaid with prewarmed DMEM containing 30 μCi of [^{3}H]thymidine per dish. After 6 h of infection the cells were put on ice and the [^{3}H]thymidine-containing medium was removed. Then the cells were washed in ice-cold PBS and subsequently overlaid with prewarmed cysteine- and methionine-free DMEM containing 50 μCi of [^{35}S]Express (NEN, Dupont) per dish. After 22 h of infection, the ^{35}S label was removed and the cells were washed in ice-cold PBS and then further incubated in prewarmed normal DMEM for 2 h. Virus purification was carried out as described below.

To assay for posttranslational processing of viral proteins, 60-mm-diameter dishes of cells were infected with VV *ts*16 at 40°C and labelled from 5 to 8 h postinfection with 50 μCi of ^{35}S label per dish. Cells were washed three times in ice-cold PBS before incubation in normal DMEM at 31°C for different periods. When appropriate, rifampin was added during the 31°C incubation at a concentration of 100 μg/ml.

Isolation of VV *ts*16 viral particles and different treatments. After 24 h of infection, cells were scraped from the dish in the medium, centrifuged, resuspended in 10 mM Tris (pH 9.0), and then lysed by passage 15 times through a 27¾-gauge needle. After low-speed centrifugation (~800 × *g*) to remove the nuclei, the supernatant was layered onto a sucrose gradient.

Different conditions for sucrose gradient purification were tested. In preliminary experiments a 12-to-26% (wt/wt) sucrose gradient in 10 mM Tris (pH 9.0) was used. The sample was centrifuged at 4°C in an SW40 rotor for 30 min at 16,000 rpm (37). This procedure was later modified to a 12-to-40% (wt/wt) sucrose gradient centrifuged at 4°C for 30 min at 16,000 rpm or a 25-to-40% (wt/wt) sucrose gradient centrifuged for 20 min at 24,000 rpm. Fractions were collected from the top of the tube, and 100 μl from each fraction was counted in a Beckman liquid scintillation counter. For the immunoblotting, equal amounts of counts were run on 15% gels and transferred to nitrocellulose. The nitrocellulose was extensively blocked by using 5% milk powder in PBS–0.1% Tween 20 and incubated with the anti-I7 antibody at a 1:1,000 dilution followed by a goat anti-rabbit antibody coupled to horseradish peroxidase (Cappel, Durham, N.C.). Enhanced chemiluminescence (ECL; Amersham, Buchler GmbH, Braunschweig, Germany) was used to visualize the protein.

For the immunoprecipitation of the core proteins, 2% sodium dodecyl sulfate (SDS) (final concentration) was added to IMVs and mutant particles from the peak fractions, and the mixtures were incubated for 30 min at 37°C. The samples were centrifuged for 5 min at full speed in an Eppendorf centrifuge, the supernatant was diluted in 1 ml of detergent solution (23), 2 μl of anti-p4a/4a (3160), anti-p4b/4b (10098Q), or anti-p28/p25 was added, and the immunoprecipitation was performed as described previously (23).

For the proteinase K treatment of isolated virus particles, aliquots from the peak fractions of the gradients were incubated with equal volumes of a 200-μg/ml proteinase K solution in 10 mM Tris (pH 9) for 30 min on ice. To stop the reaction, 1 mM phenylmethylsulfonyl fluoride was added to the reaction mixture, and the sample was quick-frozen in liquid nitrogen. The sample was thawed rapidly, and Laemmli sample buffer was added prior to SDS-polyacrylamide gel electrophoresis (PAGE) analysis as described below.

To separate core from membrane fractions, wild-type and mutant particles were briefly sonicated and then incubated for 30 min at 37°C in 1% Nonidet P-40 (NP-40) and 20 mM (final concentration) freshly made DTT. The samples were layered on top of a 75-μl 36% sucrose cushion in an ultraclear centrifuge tube (Beckman) and centrifuged in a Beckman airfuge for 30 min at 26 lb/in^2. The supernatant, containing solubilized proteins, was concentrated by acetone precipitation at −20°C, and the pellet was directly resuspended in Laemmli sample buffer.

Gel electrophoresis and autoradiography. ^{35}S-labelled material from the peak fractions was diluted in Laemmli sample buffer containing 1% SDS and 0.5% β-mercaptoethanol and electrophoresed in an SDS–15% polyacrylamide gel. Gels were processed for fluorography, dried, and exposed to X-ray film at −80°C.

RESULTS

Morphology of VV *ts*16. Prior to the biochemical analysis, we characterized VV *ts*16 by conventional Epon embedding. Figure 1 illustrates representative sections of Epon-embedded BSC40 cells infected with VV *ts*16 for 24 h under permissive conditions (31°C) (Fig. 1a) and nonpermissive conditions (40°C) (Fig. 1b). At 31°C viral structures identical to those observed in cells infected with wild-type VV could be detected: these included crescent-shaped membranes surrounding discrete foci of viroplasm, spherical immature particles in close proximity to the viral factories, and brick-shaped mature virions more in the periphery of the cell (Fig. 1a).

In agreement with earlier data (21), no normal IMVs were apparent in cells infected at the nonpermissive temperature. Instead, spherical, often asymmetrical particles accumulated in the cytoplasm. A large number of these particles contained a

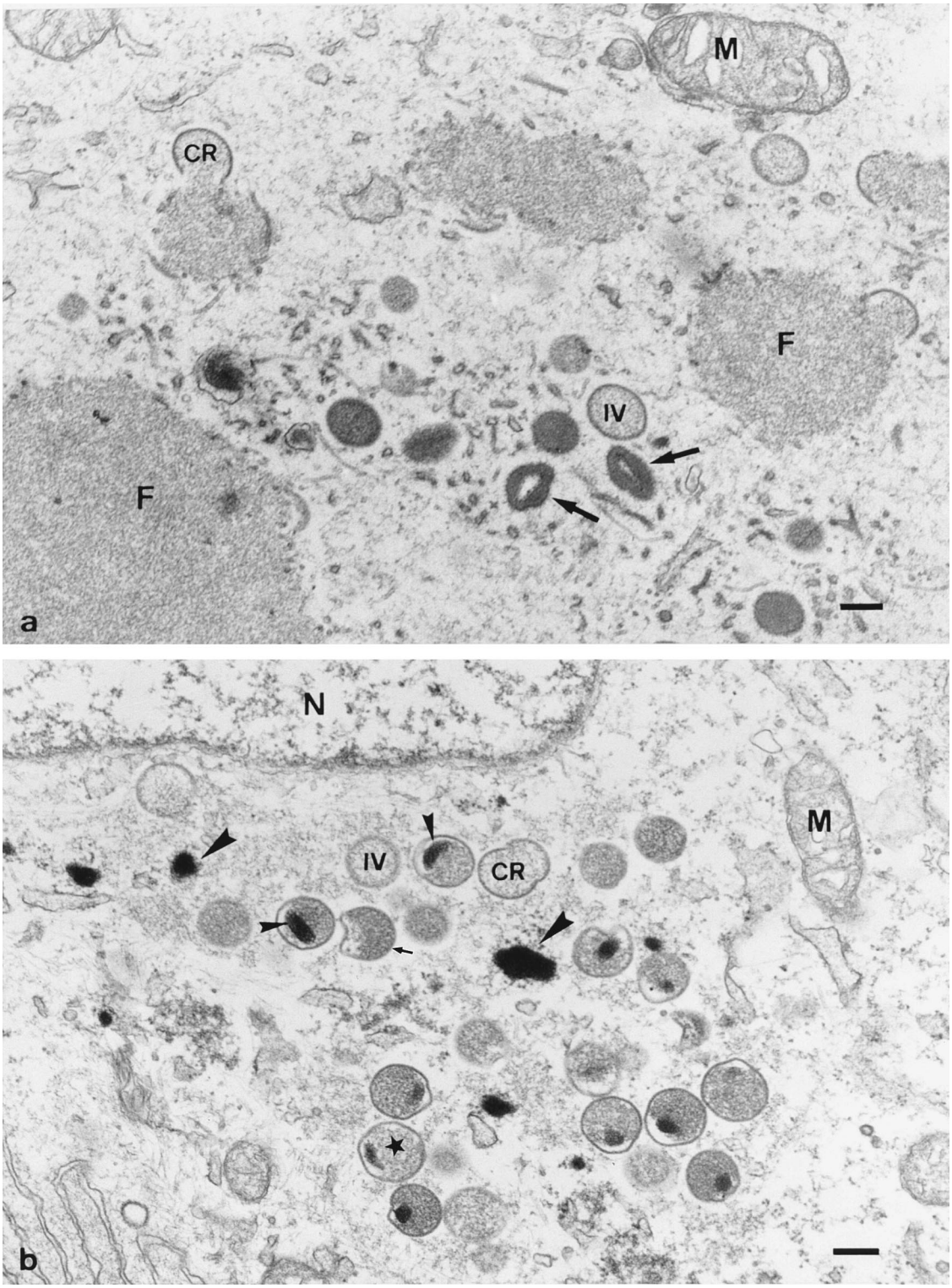

FIG. 1. Epon sections of BSC40 cells infected with *ts*16 for 24 h. (a) Cells infected at 31°C (permissive temperature) show VV at different stages of morphogenesis; the electron-dense viral factories (F) contain viral crescents (CR), spherical IV, and IMV (arrows). (b) Cells infected at 40°C (nonpermissive temperature) contain spherical particles, sometimes irregularly shaped (star), many of which contain a dense nucleoid (small arrowheads). These cells also contain viral crescents (CR), IVs, and DNA crystalloids (large arrowheads) but no IMVs. The small arrow denotes the irregular shape of some profiles of the IVs at the nonpermissive temperature. M, mitochondrion, N, nucleus. Bars, 200 nm.

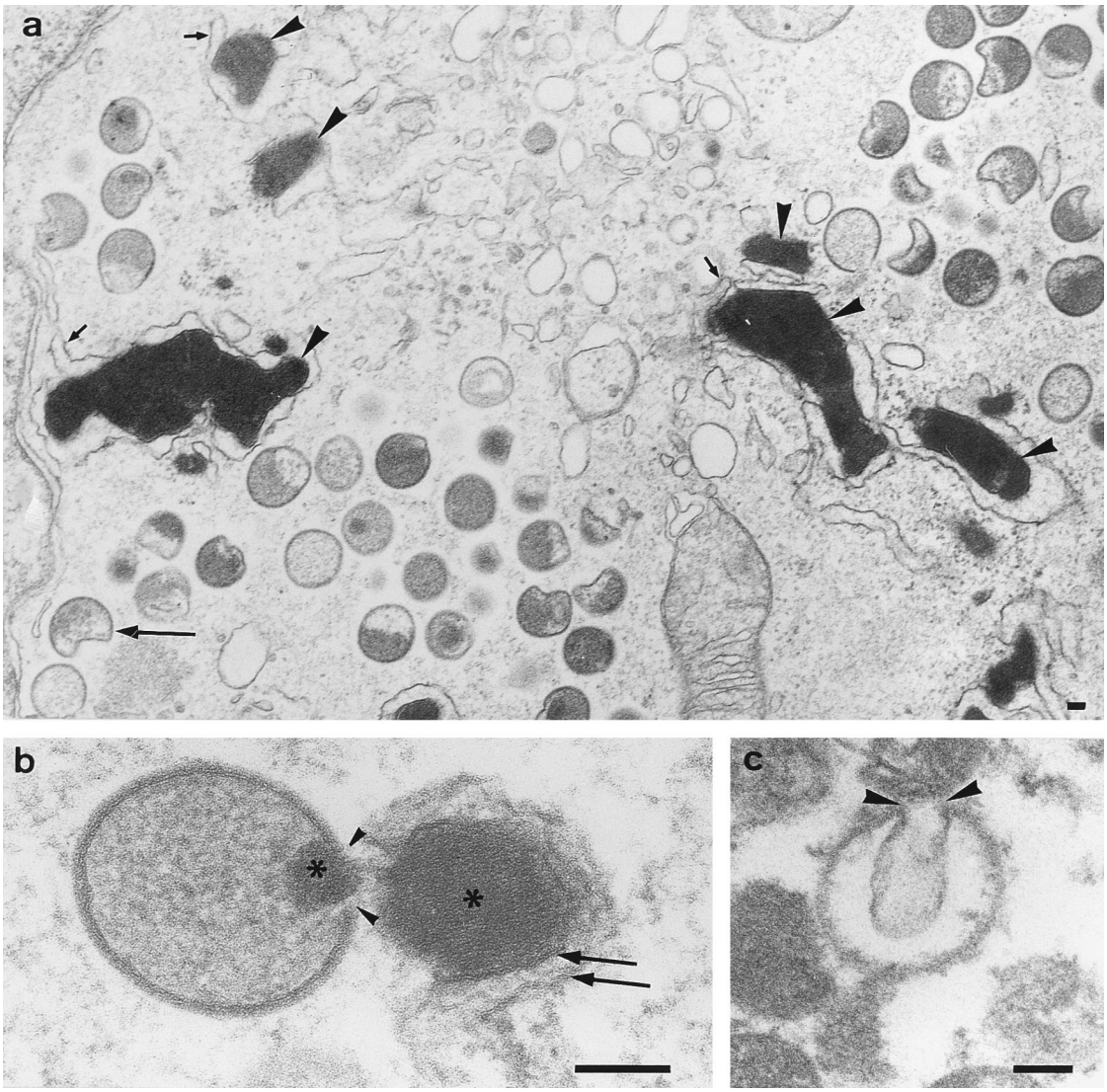

FIG. 2. (a) Epon section of a BSC40 cell infected with *ts*16 at the nonpermissive temperature for 24 h, showing the extensive accumulation of the viral DNA (arrowheads) that appears to be tightly associated with membranes of the ER (small arrows indicate ribosomes). (b) High-magnification view of the DNA (right-hand asterisk) from the same preparation, in which the parallel filaments are apparent. The two membranes that appear to enwrap the DNA are indicated by arrows. The large arrowheads and the left-hand asterisk show the site at which DNA appears to enter the IV. (c) Cryosection of a cell infected with *ts*16 for 24 h at the nonpermissive temperature and then permeabilized with SLO and incubated with DNase. The arrowheads show the points of invaginations of membrane(s) that would normally be filled with the viral DNA. Bars, 100 nm.

nucleoid and appeared to be denser than the spherical IV (Fig. 1b). At longer infection times (48 h) the particles became more irregular in shape and the envelope tended to collapse on one side of the sphere (Fig. 1b and 2a). Viral structures preceding the formation of the defective particles, such as crescent-shaped membranes and IVs, appeared to be mostly normal at the nonpermissive temperature. In Epon-embedded cells we could often see particles in which the viroplasm seemed to have condensed unevenly, leaving the particle partially empty (Fig. 1b). As discussed below, this was seldom seen with cryosections and may be an artifact of the plastic embedding.

In our extensive ultrastructural observations on VV assembly we have often noticed that the viral DNA associates closely with membranes (see also reference 13), and we suggest that this association may be important for DNA entry into the IV. In *ts*16-infected cells at the nonpermissive temperature this association of membranes with the DNA became much more evident, presumably because the entry process is arrested. At this temperature, large, filamentous aggregates of DNA accumulated, and most of them were associated with membranes after long infection times (Fig. 2a and b). In such preparations it became clear that these membranes represent the ER since they are clearly continuous with ribosome-associated membranes (rough ER). The significance of this membrane association of the DNA and its importance for the entry into the assembling VV particle must await more definitive experiments.

When the *ts*16-infected cells that had been arrested at the nonpermissive temperature were permeabilized with SLO and treated with DNase, the viral DNA was digested. In some of the defective particles the images we saw suggested that the sites previously filled with DNA were empty. For such particles we interpreted the images as suggesting that the DNA had pushed the membrane(s) into the particle, resulting in a dis-

tinct invagination (Fig. 2c; cf. Fig. 5e). The preservation of these preparations was, however, not good enough to enable us to conclude whether these invaginations possessed one or two membranes.

Figure 3 shows a panel of micrographs of the *ts*16 virus prepared under different conditions that have been selected to illuminate some features which we believe to be important for the normal assembly process and which are more easily visualized in the *ts*16 virus at the nonpermissive temperature. In Fig. 3a, which shows a cryosection of *ts*16 IVs visualized with ammonium molybdate, one IV (on the right) clearly has two membranes. These two membranes are normally so tightly juxtaposed that they appear as a single membrane (43). That they are indeed double membranes is demonstrated clearly in Fig. 3d, which shows an early step in the assembly of the IV, and more clearly in Fig. 3e, which shows an IV from a cell permeabilized with SLO and treated with proteinase K. In this image the IV shows two distinct bilayers. In a similar preparation (Fig. 3b) the structure of the DNA nucleoid is more evident following extraction of protein components. Finally, Fig. 3c shows a particle from a plastic-embedded section of a cell that was arrested for 6 h at 40°C and then switched to the permissive temperature. Although this particle is clearly abnormal it reveals structural features which are not obvious in normal IMVs; these include a peripheral cisterna, as well as the presence of at least one additional membrane bilayer around the core. The latter is electron transparent, suggesting that it does not enclose the DNA nucleoid or that the DNA was lost during specimen preparation.

Immunolocalization of viral proteins on thawed cryosections. We next analyzed VV *ts*16 infected cells using cryosections to immunolocalize the I7 protein as well as some of the major structural proteins of VV.

I7 protein. The thermosensitivity of VV *ts*16 has been mapped to the I7 gene, which encodes a 47-kDa polypeptide of yet-unknown function. The I7 protein is synthesized late in infection at both the permissive and nonpermissive temperatures, and it has been localized biochemically to the core of wild-type virions (21). In the latter study it was not determined whether the I7 protein is present in the particles that accumulate at the restrictive temperature. We therefore labelled cryosections of *ts*16-infected cells with an anti-I7 serum. In cells infected for 24 h at 31°C, viral factories were labelled, as well as the central part (viroplasm) of viral crescents and IV particles (Fig. 4a). Significant, but weaker, gold labelling was also seen on profiles of IMV particles that form at the permissive temperature (Fig. 4b). The labelling pattern resembled that found for core proteins in wild-type VV showing one or two gold particles over the central part of the IMV (41, 48). When infected cells were lysed with water for 5 min before fixation, there was a significant increase in the amount of label associated with the IV, presumably because of increased access of the antibody (Fig. 4d). Interestingly, at 40°C, labelling for I7 was present in the viral factories, but the viroplasms of the viral crescents, IVs, and the mutant particles seemed devoid of labelling (Fig. 4c). These results suggested that at the nonpermissive temperature VV *ts*16 fails to integrate the I7 protein into the particle (but see below). Experiments in which these cells at 40°C were lysed in water did not result in an increase in the labelling (not shown). In order to get a more objective impression, the gold labelling for I7 was quantitated. We compared the labelling in BSC40 cells infected at both temperatures with that in HeLa cells infected with the wild-type strain WR. As shown in Table 1, the IVs and crescents of *ts*16-infected cells had approximately six times more labelling for I7 at 31°C than at 40°C.

Collectively, these results show that the immunoreactivity for IVs in cells infected at the nonpermissive temperature is significantly lower than that seen with normal assembly intermediates.

Other viral proteins. We next undertook an extensive immunolocalization analysis to test for the presence in the mutant virus particles of proteins known to be in the IMV, using a spectrum of VV antibodies. For this we performed immunogold labelling on thawed cryosections using BSC40 cells infected with *ts*16 for 24 h at the permissive and nonpermissive temperatures.

The localization of the p14 and p32 proteins to wild-type VV has recently been described (42). The peripheral membrane protein p14 (gene A27L) is probably involved in the infection process (31–33) as well as in the wrapping of IMV by a Golgi-derived cisterna to produce the intracellular and extracellular enveloped viruses (34). We have shown by immunoelectron microscopy that in cells infected with wild-type VV, a monoclonal antibody against p14 labels the outer membrane of the IMV and an assembly intermediate between the IV and the IMV (see the introduction), whereas the IV particles are devoid of labelling (42). We rationalized this result by assuming that p14, which behaves as a peripheral membrane protein and lacks any hydrophobic stretch of amino acids long enough to span a membrane, is able to bind to a putative membrane receptor on the assembling particle only at a stage subsequent to the IV. As can be seen in Fig. 5a and b, after infection with *ts*16 at 31°C, the distribution of this antigen was comparable to that in wild-type VV, showing strong labelling of the IMVs but no labelling of IVs. In sections of cells infected with VV *ts*16 at 40°C, the mutant particles were strongly labelled for p14. The gold particles were often restricted to the irregular side of the sphere, which was irregular and flattened (Fig. 5c). In agreement with the labelling pattern seen at 31°C, the IVs and the crescents were not labelled (Fig. 5a and b).

The p32 protein (gene D8L) contains a single hydrophobic domain at its C terminus that could function as a membrane anchor (28). p32 binds to the plasma membrane of cells and is thought to have a function in virus entry (30). On cryosections of cells infected with wild-type VV, anti-p32 labelled the membranes of immature, intermediate, and IMV particles as well as additional membrane profiles in the cytoplasm (42). Essentially the same pattern was obtained when BSC40 cells were infected with *ts*16 both at the permissive (Fig. 5d) and at restrictive temperatures (Fig. 5e and f). Thus, the mutant particles appeared to contain a normal complement of p32 in their membranes.

The localization of the p65 protein (gene D13L), the target of rifampin (1, 45), during wild-type infection has also been previously examined by immunogold labelling (44). This protein is predominantly found on the inside of the forming crescents, suggesting that it might function as a part of a scaffold on the outside of the DNA-enclosing core. Although IVs and wild-type assembly intermediates are labelled strongly for p65, little labelling can be detected in mature virions; we presume that this is due to alteration or masking of the epitope. Sections of cells infected with VV *ts*16 at 31 and 40°C were labelled with a peptide antiserum (B1) raised against the COOH terminus of p65 (44). At 31°C, labelling was mainly observed on the inside of the inner membrane of viral crescents, IVs, and the intermediate form, but as with the wild-type virus, little label was detectable in the IMV (Fig. 6a). In cells infected at 40°C, crescents and IVs were labelled as expected; in addition, the most mature particles that assembled under this condition were strongly labelled, with most of the labelling being concentrated on the inner aspect of the viral membranes (Fig. 6b).

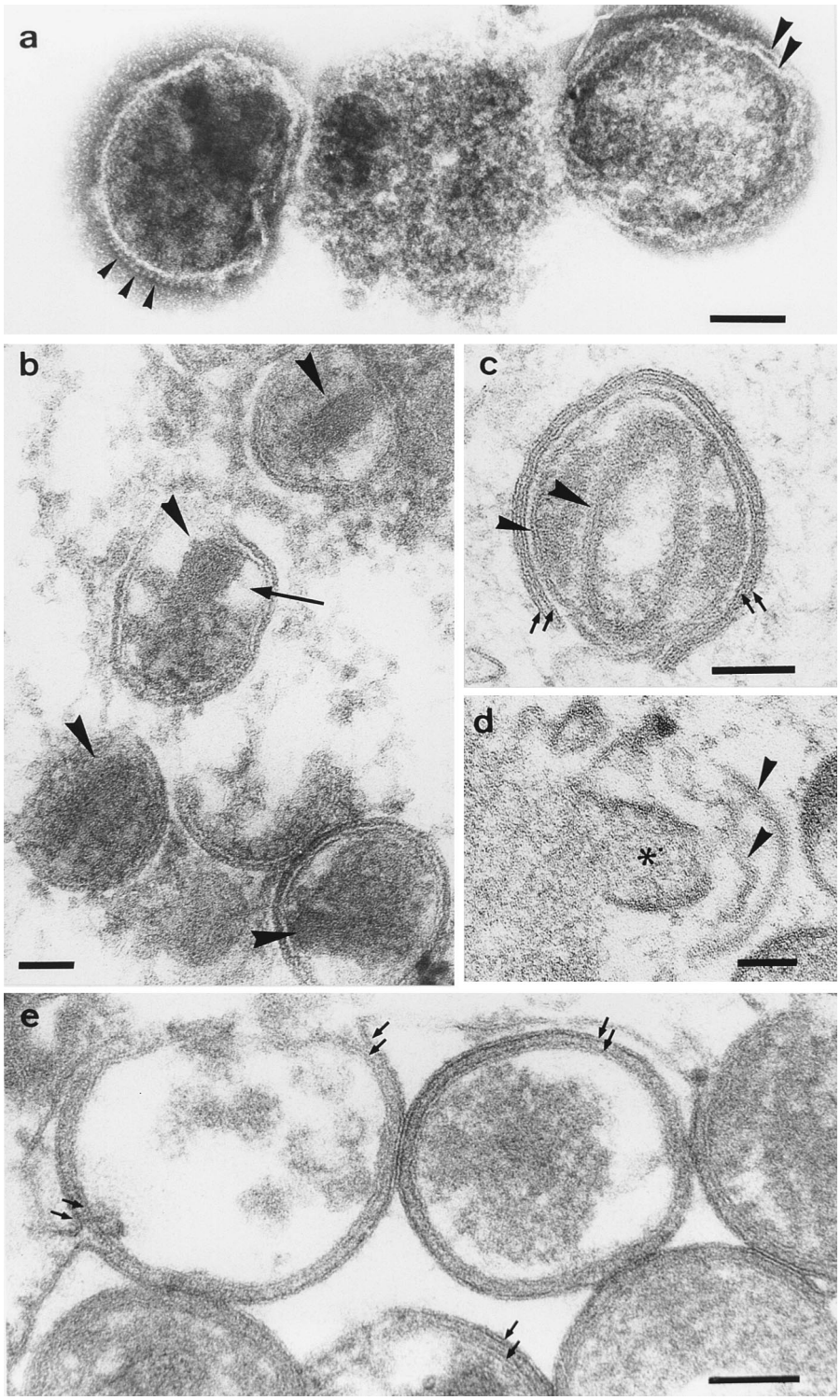

FIG. 3. Structural features of assembly intermediates in *ts*16-infected cells. (a) Thawed cryosection of a cell infected for 24 h at the nonpermissive temperature; the section was negatively stained with ammonium molybdate. The IV on the right has two membranes that are clearly separated from each other at one site (large arrowheads). In the particle on the left, the outer membrane is probably disrupted, revealing spike-like projections (small arrowheads). (b and e) IV particles from permeabilized BSC40 cells (24-h infection) that were treated with 1 mg of proteinase K per ml. (b) This treatment enhances the visibility of the viral DNA (arrowheads) by removing the bulk of the interior of the IV (arrow). (e) The two membranes of the IV (small arrows) are distinct. (c) Epon section showing a particle from a cell infected for 8 h at the nonpermissive temperature followed by a 1-h reversal to the permissive temperature. This particle, clearly abnormal, reveals a cisterna (arrows) on the periphery as well as one additional bilayer just beneath it (small arrowhead). A possible fourth bilayer indicated by the large arrowhead immediately surrounds the nucleoid, which in this case seems devoid of DNA. (d) Epon image from a cell infected for 24 h at the nonpermissive temperature to show the core (asterisk), possibly surrounded by a membrane, apparently in the process of being enclosed by a cisterna (arrowheads indicate the two membranes). Bars, 100 nm.

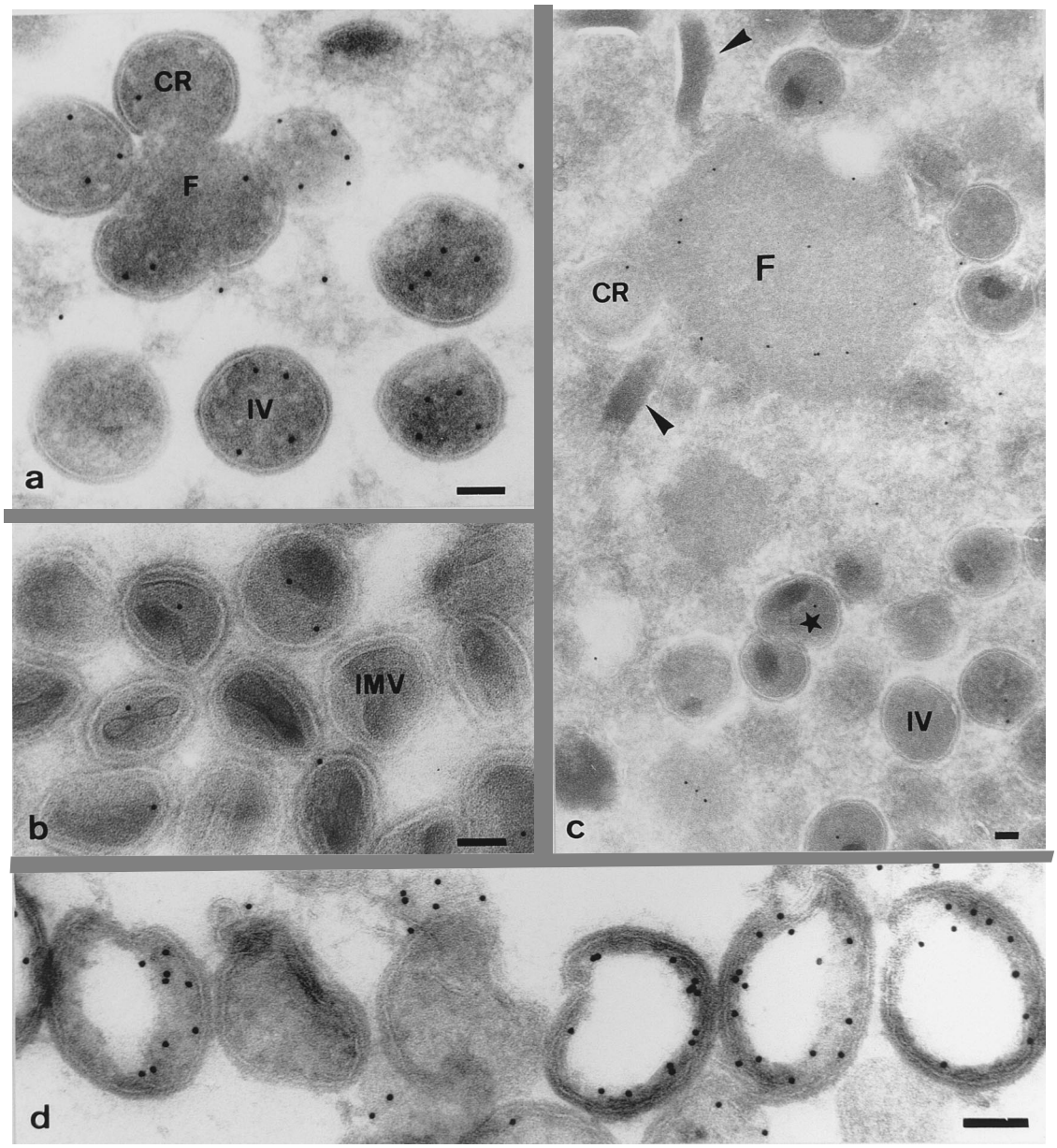

FIG. 4. Localization of the I7 protein. Cryosections of BSC40 cells infected for 24 h with *ts*16 at 31°C (a and b) and 40°C (c) and of HeLa cells infected with WR for 24 h at 37°C (d) were prepared. Sections were labelled with anti-I7 and then with 10-nm-diameter protein A-gold particles. At 31°C the anti-I7 serum significantly labels the viral crescents (CR) and IVs (a). The IMVs are labelled much less extensively: generally no more than one or two gold particles can be seen close to the core of the virion (b). At 40°C (c) the labelling is significantly weaker than at 31°C and predominantly localized to the viral factories (F). Viral crescents (CR), IVs, and the mutant virions (star) are almost totally devoid of labelling. Note the presence of small DNA crystalloids in close proximity to the viral factory (arrowheads). When HeLa cells infected with wild-type VV were incubated for 5 min in water before fixation followed by cryosectioning and immunolabelling, most of the IVs appeared empty but were labelled very strongly with the I7 antibody (d). Bars, 100 nm.

As described earlier for the IV of the wild-type virus, some gold particles were also seen on the outside of the viral particle: it should be noted that the size of the protein A-gold-antibody complex (~20 nm in length) is too large to enable us to be confident that this labelling indeed represents antigen on the particle surface. The fact that no labelling could be detected on the surface of isolated, negatively stained virions with this antibody (see below) argues against the presence of significant amounts of p65 on the outer surface.

The proteins 4a, 4b, and 25K (genes A10L, A3L, and L4R, respectively) are associated with the core of mature virions (35,

TABLE 1. Quantitation of VV I7 in BSC40 cells infected for 24 h with *ts*16 or WR

Virus strain	Infection temperature (°C)	Density of immunogold particles (mean ± SD)[a]	
		IV and CR	IM and IMV
*ts*16	40	0.39 ± 0.61	0.44 ± 0.62
*ts*16	31	2.39 ± 1.72	1.28 ± 1.07
WR	37	3.06 ± 2.26	1.44 ± 1.25

[a] Number of gold particles per square micrometer of micrograph. CR, crescent; IM, intermediate.

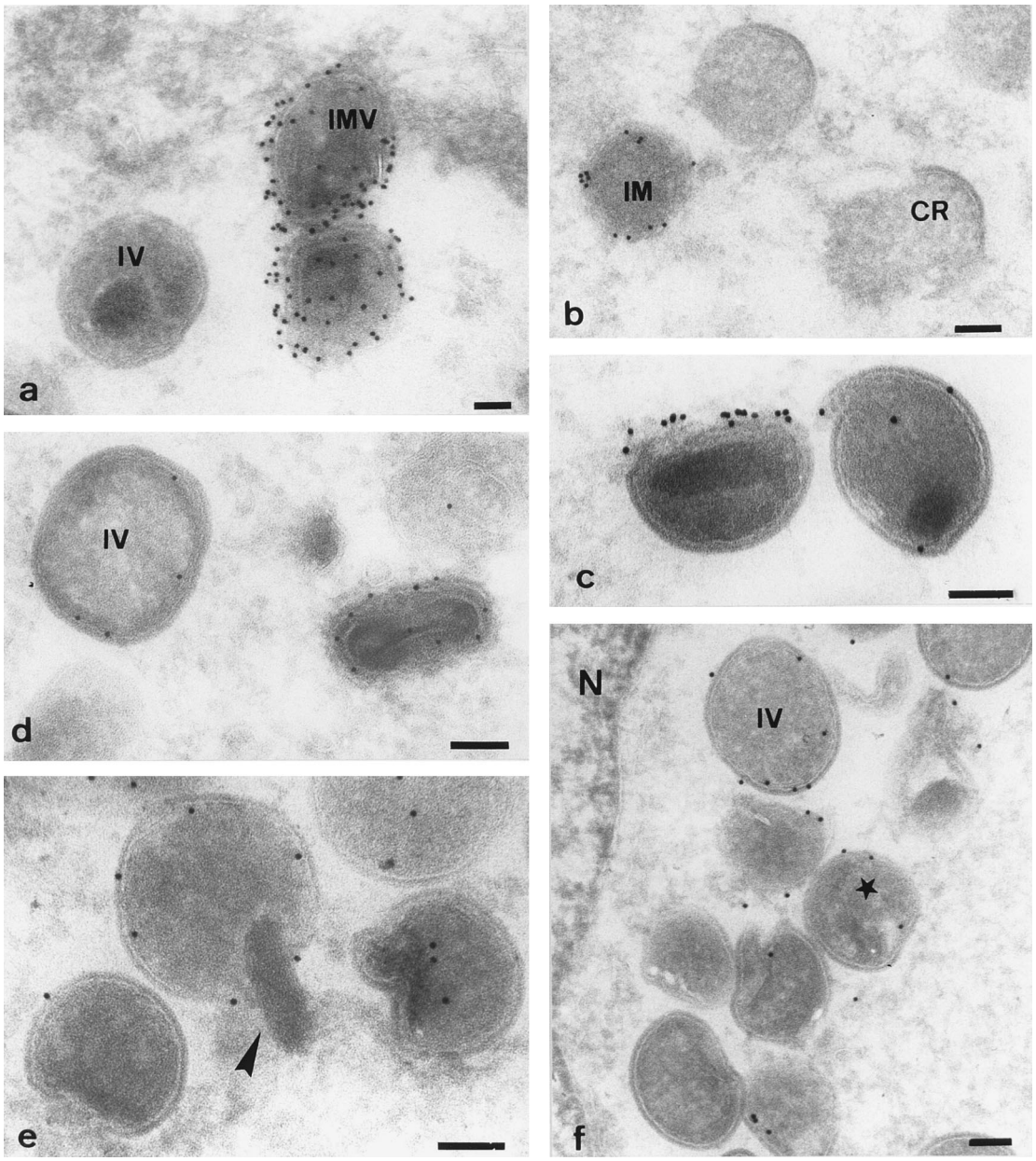

FIG. 5. Immunolocalization of p14 and p32 in cryosections of BSC40 cells infected with *ts*16 for 24 h at 31°C (a, b, and d) and 40°C (c, e, and f). The sections were labelled with either a monoclonal antibody specific for p14 (a to c) or a rabbit antiserum directed against p32 (d to f). At 31°C anti-p14 strongly labels the outer membrane of IMV (a) and the assembly intermediates (IM) (b). Viral crescents (CR) (b) and IVs (a) are not labelled. At 40°C anti-p14 labels the accumulated mutant virions strongly, often on the more irregular part of the outer membrane (c). Anti-p32 labels IMVs as well as IVs on the outer membrane at 31°C (d). At 40°C anti-p32 labels the membranes of the IVs and mutant virions (star) (f). Note the virion in panel e that is in the process of taking up the DNA (arrowhead). N, nucleus. Bars, 100 nm.

46, 50–52). Immunogold labelling with rabbit antisera against the three proteins gave very similar results and can be described collectively. Gold particles were evenly distributed in the viroplasm of the *ts*16 particles and in the viral factories under restrictive conditions, as was also seen in IVs during wild-type infections (Fig. 6c). Again, IMVs were labelled sparsely (results not shown). As for the p65 protein and the I7 protein, the failure to detect significant amounts of label for these proteins in the IMV core might be due to the fact that the antigens are not accessible in the densely packed IMV.

Labelling with anti-DNA antibodies confirmed that the dense nucleoids observed in the *ts*16 particles that accumulated at the restrictive temperature by using Epon embedding (Fig. 1) represented DNA (Fig. 6d). Labelling could also be detected on the larger crystalloids of DNA (data not shown) as well as on smaller structures of dense material in the cytoplasm, possibly representing smaller fragments of DNA ready to enter a viral particle (not shown). The fact that not all the DNA structures in profiles of the defective particles were labelled with anti-DNA (Fig. 6d) is probably due to their inaccessibility to antibody and to the fact that only the DNA appropriately exposed on the surface of the thawed cryosection will be labelled.

To summarize these results, most of the viral antigens ap-

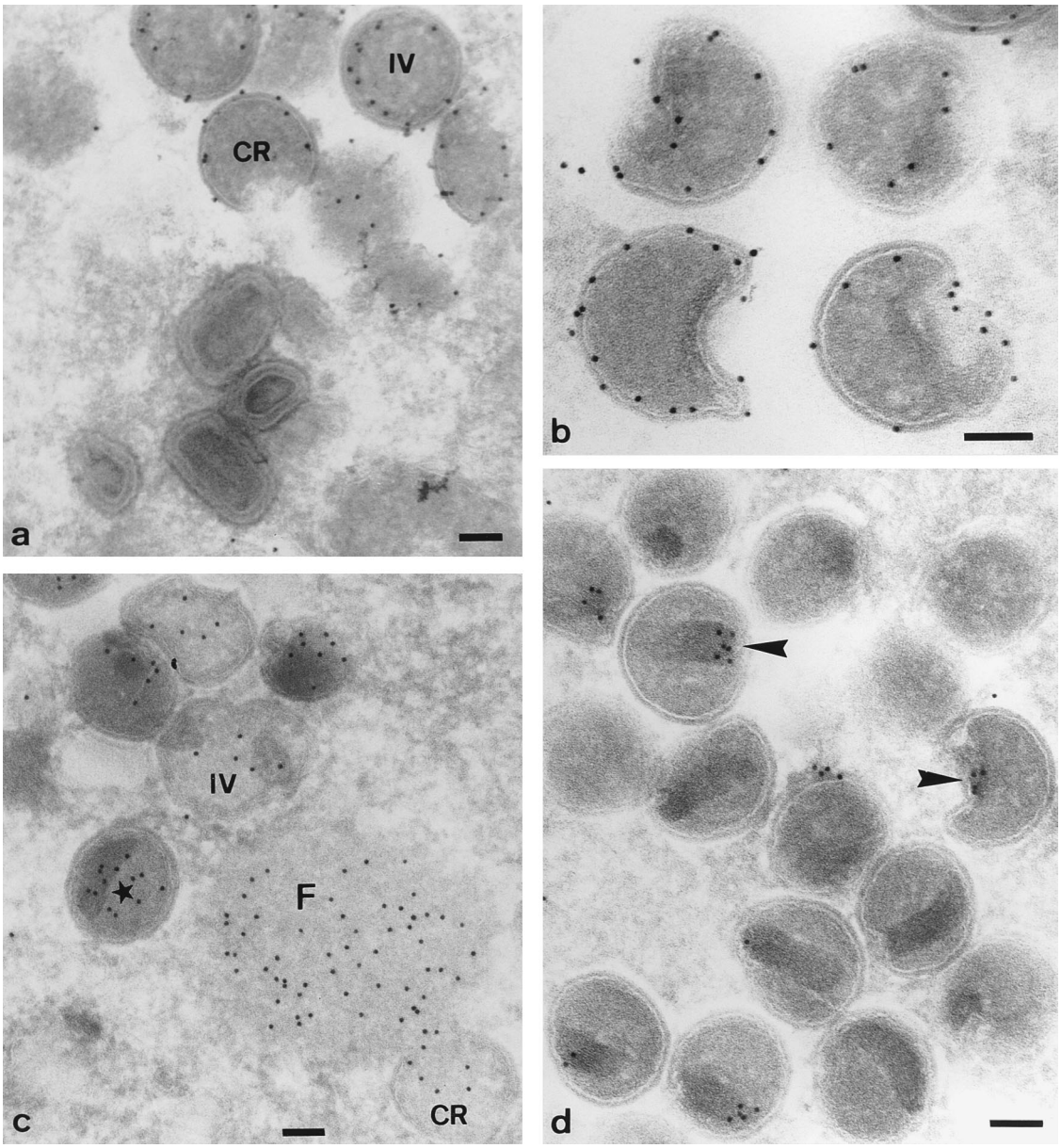

FIG. 6. Immunolocalization of p65, p4a/4a and the viral DNA in cryosections of BSC40 cells infected with *ts*16 at 24 h after infection. Sections of cells infected at 31°C (a) and 40°C (b) were labelled with antibodies against p65. At 31°C most but not all of the labelling is found on the inner side of the inner membranes of the IVs and the crescents (CR). IMVs are devoid of labelling. At 40°C the mutant virions are labelled similarly to the IVs, predominantly around the inner side of the inner membrane (b). (c) Immunolocalization of p4a/4a of cells infected at 40°C. Cryosections were labelled with an antibody recognizing both the precursor and the processed form of 4a. Anti-p4a/4a strongly labels the viral factories (F), the inside of the viral crescents, IVs, and the mutant virions (star). (d) Anti-DNA antibody labels the dense nucleoids (arrowheads) in the virions that accumulate at 40°C. In some virions the dense nucleoid that is clearly visible is not labelled, probably because of inaccessibility of the DNA to the antibody. Bars, 100 nm.

peared to localize to the mutant particle as expected for the assembly intermediate between the IV and the IMV, with two exceptions. The labelling for p14 was often polarized on one side of the particle, while no labelling for the I7 protein was evident in the defective particles.

Arrest of assembly of VV *ts*16 is not reversible. One important question was whether the spherical particles that accumulated at the nonpermissive temperature would form normal brick-shaped IMVs after being shifted to the permissive temperature. To investigate this, cells were infected at 40°C for 12 h and then shifted to 31°C and chased for up to 8 h in the presence of rifampin. Rifampin specifically inhibits VV assembly at a stage before formation of the crescents and is not known to have any effect on the maturation step leading from the IV to the IMV (13, 26, 27). Rifampin was added to block the putative formation of IMVs from remaining protein pools inside the cells. Despite a careful analysis of thin sections of such pulse-chased cells, no mature virions could be detected, suggesting that the *ts*16 particles which accumulated at 40°C do not mature into normal IMVs (Fig. 3c). In contrast, cells that were infected at the permissive temperature in the presence of rifampin formed normal amounts of IMV after washout of the drug (data not shown). Further evidence that the particles that accumulated at the nonpermissive temperature were irrevers-

ibly arrested came from the biochemical analysis of purified particles labelled under the pulse-chase conditions described above (see Fig. 9, lane C; see also below).

Isolation of *ts*16. In order to further characterize the spherical particles that accumulated at the restrictive temperature, we next attempted to purify them from infected cells. Initially we used a simplified version of the procedure described by Sarov and Joklik (36) to isolate intermediates of VV assembly. *ts*16-infected BSC40 cells were labelled with [^{3}H]thymidine and with ^{35}S, chased for 2 h in unlabelled medium, and homogenized. The homogenate was centrifuged gently to remove the nuclei, and the supernatant was layered onto a 12-to-26% (wt/wt) sucrose gradient and centrifuged for 30 min at 16,000 rpm in an SW40 rotor. Under these conditions one peak of radioactivity containing both [^{3}H]thymidine and ^{35}S label could be detected close to the bottom of the gradient, at both permissive and nonpermissive temperatures. Since our initial goal was to establish gradients that would separate the defective particle from the IMV, we modified the conditions in the following way. Cells were infected, labelled, and homogenized as described above. The supernatants were analyzed on either 12-to-40% (wt/wt) or 25-to-40% (wt/wt) sucrose gradients that were centrifuged for 30 min at 16,000 rpm or for 20 min at 24,000 rpm, respectively, in an SW40 rotor. Both sets of conditions gave similar results. Figure 7 shows the distribution of ^{3}H and ^{35}S labels over 12-to-40% gradients at 31 and 40°C. At both temperatures one peak, containing labelled DNA and protein, was detected at a position near the bottom of the gradient. Apparently, under the conditions used, we were unable to separate the IMV from the defective *ts*16 particles that accumulate at the nonpermissive temperature.

Characterization of the isolated particles. In order to analyze the particles found in the peak of ^{35}S and ^{3}H in the gradients in more detail we first performed a negative-staining EM analysis. As expected, brick-shaped particles, indistinguishable from isolated wild-type IMVs (Fig. 8c and e), were present in the peak obtained after infection at the permissive temperature. Consistent with the images obtained with Epon embedding and cryosections, at the nonpermissive temperature, the isolated particles had a spherical appearance with a diameter of about 270 nm. No brick-shaped virions could be seen in this fraction (Fig. 8a, b, d, and f). In some views it was evident that these particles were not complete spheres but had an indentation at one pole (Fig. 8b), in agreement with the analysis with thin sections (Fig. 2a and c).

Labelling with antibodies was carried out on these whole, isolated particles to examine which antigens were exposed on their surfaces. After labelling, the particles were negatively stained and examined by EM. The results of these experiments are illustrated in Fig. 8. The p14 antibody gave a very strong labelling on the mature IMV isolated from cells infected at the permissive temperature (Fig. 8c). At the nonpermissive temperature the isolated defective particles showed a variable labelling: some were labelled strongly, especially on one pole (Fig. 8d), while others seemed devoid of labelling (data not shown). This finding is consistent with the results from the immunolabelling on cryosections, where the labelling was mostly concentrated on one side of the particle.

Antibodies against the membrane protein p32 extensively labelled the outside of both mature virions and the defective particles (Fig. 8e and f). No significant labelling could be detected on the outer surfaces of these particles for I7, p65, or the core proteins 4a, 4b, and 25K (data not shown).

Protein composition of the isolated particles. *ts*16 has been classified as belonging to a group of mutants with wild-type protein and DNA synthesis (3). This finding was based on

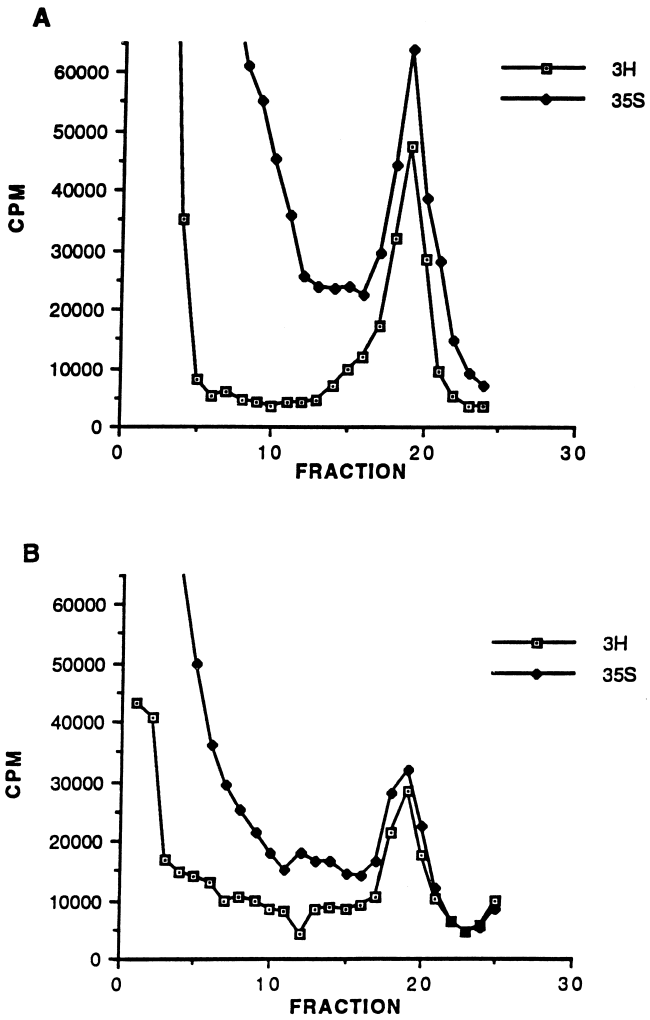

FIG. 7. Purification of VV *ts*16 on sucrose density gradients from BSC40 cells infected for 24 h under permissive (A) and nonpermissive (B) conditions. Infected cells kept at either temperature were labelled with [^{3}H]thymidine (3H) from 1 to 5 h postinfection and with ^{35}S label (35S) from 5 to 22 h postinfection. Postnuclear supernatants of infected cells were layered onto a continuous sucrose gradient and centrifuged for 30 min at 16,000 rpm in an SW40 rotor. Fractions were collected from top to bottom, and radioactivity was counted.

SDS-PAGE of pulse-labelled, infected cells grown at 40 and 31°C. We next analyzed by SDS-PAGE the protein composition of the defective particles, isolated as described above. The protein patterns of *ts*16 grown at 31 and 40°C were compared with that of purified IMV. As expected, the protein pattern of *ts*16 grown at 31°C was identical to that of purified IMV (not shown). The composition of the defective particles, however, appeared to be different. The most striking difference was that the core proteins p4a, p4b, and p25 were in the uncleaved precursor form and now appeared as bands of 95, 65, and 28 kDa, respectively (Fig. 9, lane B; Fig. 10). As shown by immunoprecipitation, at the permissive temperature the proteins migrated mainly as 62-, 60-, and 25-kDa bands, which correspond to the sizes of the proteolytically cleaved products (Fig. 10) (26, 47, 49). Also, the relative abundance of some of the proteins in the defective particles appeared to be different from the abundance in the virus from cells infected at 31°C and that in wild-type IMV. Another striking difference was that in the defective particles there was an abundant band migrating

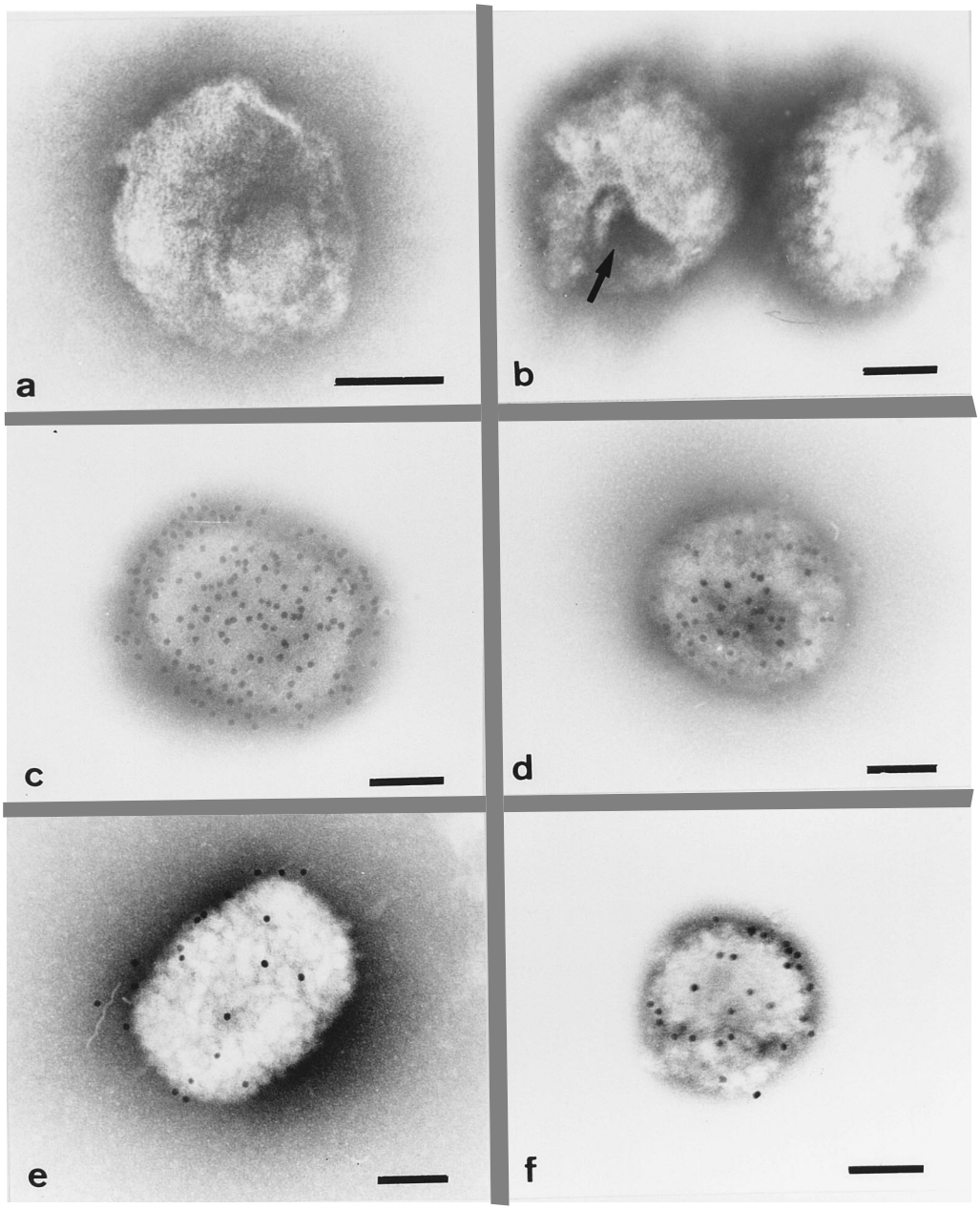

FIG. 8. Negative staining and immunogold labelling of sucrose-purified VV *ts*16 virions made at 31 and 40°C. Brick-shaped virions (c and e) were isolated from cells infected under permissive conditions, while spherical particles (a, b, d, and f) were obtained from cells infected under nonpermissive conditions. Some particles obtained from infected cells kept at 40°C are irregularly shaped and often have an indentation on one side (arrow in panel b). p14 (c and d) and p32 (e and f) are localized to the surface of the isolated particles in both IMV (c and e) and the mutant particle (d and f). Bars, 100 nm.

around 24 kDa while in the IMV a similar band seemed to run at about 20 kDa (Fig. 9, lanes B and C). The identity of this band was not further investigated.

To assess whether the I7 protein was present in the mutant particles, the labelled peak fractions of the gradients were run on SDS-PAGE and blotted onto nitrocellulose. Care was taken to load the same amount of radioactive counts of the particles isolated from cells infected at 31°C and those infected at 40°C. As a control, we also used labelled wild-type IMV, using five times more counts. To our surprise, and in obvious disagreement with the EM data, the I7 protein appeared to be present in roughly similar amounts in the mutant particles and in the viruses isolated from cells infected at the permissive temperature (Fig. 11). The I7 protein in the mutant particles, however, appeared to migrate slightly faster. The reason for this faster migration is at present not understood.

We further investigated whether the protein precursors that had accumulated during infection at 40°C would be processed following a temperature shift down to 31°C. BSC40 cells infected and labelled with ^{35}S for 24 h at 40°C were washed and then shifted to 31°C for various periods in the presence and absence of rifampin (see above). After the temperature shift, all three core proteins appeared to remain uncleaved (Fig. 9, lane C), in agreement with the EM data showing that the

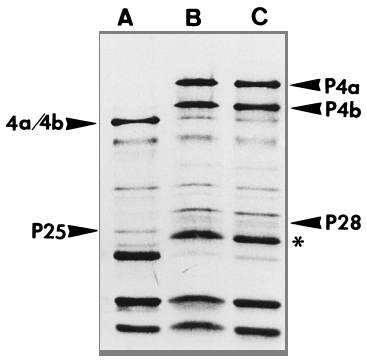

FIG. 9. Protein composition of ^{35}S-labelled and sucrose gradient-purified particles from BSC40 cells infected at permissive (lane A) and nonpermissive (lane B) temperatures. The purified particles were run on SDS–15% PAGE. In the particles isolated from cells kept at the nonpermissive temperature, the major core proteins (4a, 4b, and p25) are in their precursor forms (indicated for lane C by arrowheads), while the particles isolated from cells infected at the permissive temperature contain only the processed forms of these proteins (arrowheads beside lane A). Note also the band around 24 kDa (asterisk), which is present only in particles from cells infected at the nonpermissive temperature (lanes B and C), while a corresponding band running at about 20 kDa is present at the permissive temperature (lane A). Lane C, particles isolated from cells infected and labelled with ^{35}S at 40°C and then chased at 31°C for 6 h in the presence of 100 μg of rifampin per ml. The protein pattern in lane C is identical to that in B and shows that the core proteins have not been processed under these conditions.

particles that accumulate at the nonpermissive temperature are irreversibly arrested in their assembly. These findings are in agreement with earlier data showing that processing of the major core proteins coincides with the late morphological changes that occur during the formation of the IMV (26) and argue that at the nonpermissive temperature the *ts*16 particle is arrested before this processing stage.

The mutant particles may lack a core. Not much is known about the formation of the VV nucleocapsid, or core. It is assumed that the entry of the DNA into the IV somehow triggers the proteolytic cleavage of the core proteins and the formation of a core structure. This in turn coincides with the morphological change from the spherical IV to the brick-shaped IMV, a shape that may be determined by a underlying core structure. The VV core has been operationally defined as a structure remaining after extraction of IMV with NP-40 and a reducing agent (10, 16, 17, 37) or as an intermediate of disassembly during VV infection (15, 38). The classical assay to isolate cores consists of incubating IMV in NP-40 with β-mercaptoethanol or DTT at 37°C, after which the membrane and membrane-associated proteins can be separated from the insoluble (brick-shaped) core by simple centrifugation (see above references). We therefore asked whether the *ts*16 particles that accumulate at the restrictive temperature would behave similarly under these conditions. As expected from earlier studies upon incubation of particles made at 31°C with 1% NP-40 and 20 mM DTT, a membrane fraction that mainly consisted of 4a/4b, p25, and p11 could be separated from a core fraction (see also reference 17). Upon incubation of the defective particles, however, no insoluble core fraction could be centrifuged down. Instead all the proteins were now soluble in NP-40–DTT (Fig. 12). An exception, however, was a protein migrating as an 11-kDa species, some of which could be detected in the pellet.

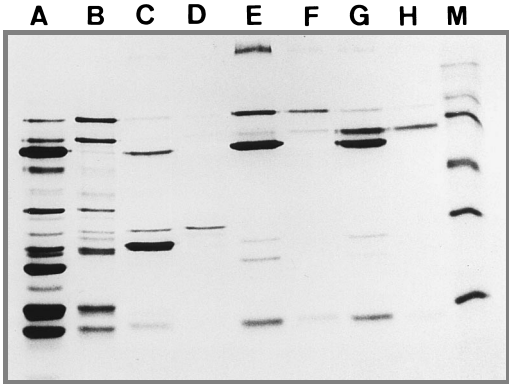

FIG. 10. Immunoprecipitation of p4a/4a, p4b/4b, and p28/p25 from IMVs and mutant particles. Lanes A and B, particles isolated from *ts*16-infected cells at 31 and 40°C, respectively. These particles were dissolved and immunoprecipitated with anti-p28/p25 (lanes C and D), with anti-p4a/4a (lanes E and F), and with anti-p4b/4b (lanes G and H) at 31°C (lanes C, E, and G) and 40°C (lanes D, F, and H). Lane M, ^{14}C marker. Although the antibodies immunoprecipitate bands of the expected size, they also appear to coimmunoprecipitate to variable extents the other core proteins. Note also that while at 40°C the three core proteins are quantitatively in their unprocessed precursor forms, at 31°C most but not all of these proteins are processed.

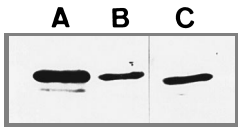

FIG. 11. The I7 protein is present in wild-type IMVs (lane A) and in particles isolated from VV *ts*16-infected cells at the permissive (lane B) and nonpermissive (lane C) temperatures. ^{35}S-labelled IMV and the peak fractions from virions isolated as described for Fig. 5a and b were run on SDS-PAGE and blotted onto nitrocellulose. About five times more counts were loaded for the wild-type IMV than for the others, while for the peak fractions from Fig. 5a and b equal counts were applied. The nitrocellulose was incubated with the I7 antibody at a 1:1,000 dilution, and the proteins were detected by enhanced chemiluminescence. Only the relevant part of the blot is shown.

These results suggest that the detergent- and DTT-insoluble core structure that is found in the IMV has not yet assembled in the *ts*16 particles that accumulate at the nonpermissive temperature. Alternatively, the *ts*16 particles possess a core that, however, does not resist the NP-40–DTT treatment.

The defective VV *ts*16 particles are not completely sealed. While the IMV is clearly a tightly sealed particle, the crescents

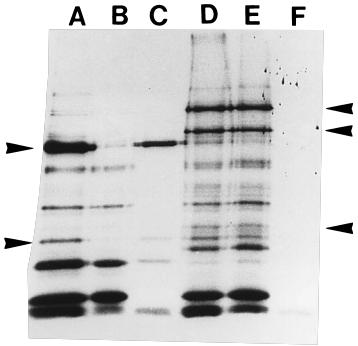

FIG. 12. *ts*16 defective particles lack an insoluble core fraction. ^{35}S-labelled and sucrose-purified mutant and wild-type particles were treated for 30 min at 37°C with 1% NP-40 and 20 mM DTT. The soluble and insoluble fractions were separated by centrifugation. Lanes A through C, particles isolated from cells kept at 31°C; lanes D through F, particles from 40°C infections. Lanes A and D, untreated particles; lanes B and E, detergent-soluble fractions; lanes C and F, insoluble fractions. Note that in the mutant particles only a faint band around 11 kDa can be detected in the insoluble fraction (lane F). The arrowheads point to the positions of the core proteins, p4a/4a, p4b/4b, and p28/p25 (top to bottom).

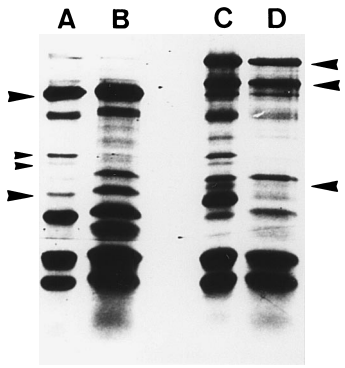

FIG. 13. Isolated *ts*16 defective particles are not completely sealed. ^{35}S-labelled and sucrose-purified wild-type and mutant particles were treated with 100 μg of proteinase K per ml for 30 min on ice and run on SDS–15% PAGE. Lanes A and C, control lanes containing untreated IMV and defective particles, respectively. Proteinase K treatment results in the digestion in the wild-type IMV of proteins running at 32 and 35 kDa (small arrowheads), while the core proteins are completely protected (lane B, large arrowheads). In the defective particles, in addition to the two membrane proteins, the core proteins 4a and 4b are partially digested, while the p25 protein is completely lost (lane D, arrowheads).

and IVs are open to the cytoplasm (43). It was thus of interest to find out whether the intermediate particles which accumulate in *ts*16 at the nonpermissive temperature were still open or whether they had matured beyond the stage at which the particles seal. For this the isolated mutant particles were treated with proteinase K (100 μg/ml) for 30 min on ice, after which the protein pattern was compared with that of untreated virions by SDS-PAGE. If particles are sealed, only proteins exposed on the surface of the virion would be expected to be accessible to the protease. As is evident in Fig. 13, virions made at the permissive temperature clearly lost proteins migrating at 35 and 32 kDa, while the core proteins were protected (18). In contrast, virions made at the nonpermissive temperature lost not only p35 and p32 but also the core proteins; p28 was completely lost, while p4a and p4b appeared partially digested. These results indicate that these particles were not completely sealed. That the particle is not as open as are the IVs was also suggested by a protease experiment using permeabilized cells (43). At the nonpermissive temperature, protease enters the permeabilized cells, as is evident by loss of the cytoplasmic and nucleoplasm density. However, the defective particles were only partially digested, as is evident by the presence of electron-dense material. In some of these images the periodic packed nature of the DNA is especially evident (Fig. 3b).

DISCUSSION

As a part of our effort in understanding how VV assembles we focused here on the characterization of *ts*16, a mutant virus that at the nonpermissive temperature is arrested at an interesting stage of its assembly. As shown by Kane and Shuman (21), and in more detail in this study, the block in assembly coincides with the complex morphological transition from the spherical IV, which does not contain DNA, to the brick-shaped IMV, in which the genome is fully enclosed in a sealed particle. In the normal assembly process this stage is relatively rare, which suggests that it is a relatively short-lived intermediate (13, 42).

Our extensive EM analysis of the assembly of wild-type VV has led us to believe that the viral DNA is packaged into a preformed nucleoid before it enters the viral particle and that these nucleoids may associate with cellular membranes prior to entry (see also reference 13). Many images of the *ts*16-infected cells at the nonpermissive temperature support this view and provided us with interesting images of the viral DNA and its possible entry process. From early on in our EM studies of VV assembly we had noticed that a small but consistent fraction of the viral DNA is present in roughly brick-shaped nucleoids that are tightly bound to cellular membranes. Some of these cisternae show above-background labelling for markers of the intermediate compartment (unpublished data) which we consider a specialized domain of the ER (22). The block in assembly of the mutant virus seemingly led to an exaggeration of one feature of the normal entry process, namely, the binding of the DNA nucleoids to membranes of the ER; in addition the DNA builds up large aggregates, as occurs following rifampin treatment (13). Further studies will be needed to determine whether this membrane association is essential for the DNA entry process.

It is intriguing that the protein which has undergone a point mutation in the *ts*16 virus is I7, a protein with partial homology with the type II topoisomerase of *S. cerevisiae* (21). Kane and Shuman logically suggested that the mutation in this protein affected the ability of the DNA to be properly packaged, leading to the block in assembly. Our data are consistent with, but do not prove, this hypothesis. During normal assembly the I7 protein, like all the core proteins we have examined, localizes to the central matrix of the IV before the DNA enters the particle, as determined by immunogold labelling. As is the case for many core antigens, the density of labelling is significantly reduced in the core of the IMV relative to that in the IV, most likely for steric reasons. In the *ts*16 virus at the nonpermissive temperature the labelling for the I7 protein of the IV, as well as the most developed intermediate forms that accumulate under this condition, is reduced to levels that are only slightly above background. However, immunoblotting analysis of the isolated mutant particles shows that the I7 protein is detected in the particle in amounts similar to those found in the IMV. Together, these data argue that the mutated protein can enter the assembling virion but in a form that poorly recognizes its antibody on the surface of formaldehyde-fixed, thawed cryosections. Presumably, the structural change induced by the mutation also impairs its proposed function in packaging the viral DNA. Whether or not this theory is correct, our morphological analysis argues strongly that the assembly block coincides with a critical stage in the entry of the DNA.

The intermediate stage at which the *ts*16 virus is blocked at the nonpermissive temperature is clearly more advanced in its assembly than is the IV, although at first glance both particles look similar. Thus, whereas random sections through the IVs invariably give rise to spherical profiles (although the particles are completely open and their contents completely digested with protease [43]), many profiles through the *ts*16 mutant particles are hemispherical at one pole only. In this study the three-dimensional appearance of these particles was best appreciated by the negative-staining EM approach, which showed that, when the orientation was favorable, these particles resembled a sphere with an indentation at one pole. From thin-section analysis it seems tempting to suggest that this indentation reflects the site at which the DNA enters the particle. Biochemically, as assayed by protease digestion of the isolated particles, the particles seemed partially open. In agreement with these data the EM analysis suggests that only a part of the electron-dense material around the DNA was sensitive to protease attack, unlike the IV, whose contents are essentially completely digested (see also reference 43).

While the *ts*16 particles are irreversibly arrested in their development, a number of proteins appear to be localized in a

manner indistinguishable from that in normal VV. Thus, besides the core proteins already mentioned earlier, p32, an outer membrane protein of IMV which is normally localized to the outer membrane of the crescents and IVs (42), shows the same uniform membrane localization in the *ts*16 particle at the nonpermissive temperature. Further, the p65 protein that genetic studies argue to be the target of rifampin localizes to the inner membrane of the spherical IV (44) as well as that of the defective *ts*16 particles. An interesting difference from the normal assembly process involved the peripheral membrane protein p14. This protein, which is an abundant component on the outer surface of the IMV, is not detected by immunogold labelling on the crescents or IV but is acquired in what appears to be a distinct step in the normal assembly process, the intermediate particle between the IV and the IMV (42). Such particles appear to be uniformly labelled with anti-p14 antibodies. Rodriguez et al. (31) have proposed that p14 binds to the integral membrane protein p21. The latter is therefore a candidate for being the receptor that might be activated for binding p14 only at the intermediate particle stage. The *ts*16 particle is clearly arrested at, or near, this intermediate stage since it is labelled strongly for p14 both on sections and on the outside of the isolated particles by negative staining. However, the distribution of label is abnormal in that p14 is clearly concentrated on some parts of the particle and depleted in others. We presume that this difference is somehow related to the defect in assembly, but further studies will be required to determine its significance. In contrast to labelling for p14, in preliminary studies antibodies to its putative receptor p21 label the membranes of the mutant particles in a uniform manner on sections (not shown).

The Condit collection of *ts* mutants of VV includes a number of examples in which a known protein is mutated and, as a result, a key step of assembly or disassembly of the virus is blocked. We believe that the combined morphological and biochemical analysis used here to characterize the *ts*16 mutant will continue to be a powerful approach to characterize other temperature-sensitive mutants with the expectation that these could open up key insights into the mechanisms of VV assembly and disassembly.

ACKNOWLEDGMENTS

We thank M. Esteban, E. Niles, D. Hruby, and R. Doms for antibodies.

J.K.L. was supported by a fellowship from the Human Frontier Science Program.

REFERENCES

1. **Baldick, C. J., and B. Moss.** 1987. Resistance of vaccinia virus to rifampicin conferred by a single nucleotide substitution near the predicted NH2 terminus of a gene encoding an Mr 62,000 polypeptide. Virology **156:**138–145.
2. **Cairns, H. J. F.** 1960. The initiation of vaccinia infection. Virology **11:**603–623.
3. **Condit, R. C., and A. Motyczka.** 1981. Isolation and preliminary characterization of temperature-sensitive mutants of vaccinia virus. Virology **113:**224–241.
4. **Condit, R. C., A. Motyczka, and G. Spizz.** 1983. Isolation, characterization, and physical mapping of temperature-sensitive mutants of vaccinia virus. Virology **128:**429–443.
5. **Dales, S.** 1963. The uptake and development of vaccinia virus in strain L cells followed with labelled viral deoxyribonucleic acid. J. Cell Biol. **18:**51–72.
6. **Dales, S., and B. G. T. Pogo.** 1981. Biology of poxviruses. Virology Monogr. **1981:**54–61.
7. **Dales, S., and L. Siminovitch.** 1961. The development of vaccinia virus in Earle's L strain cells as examined by electron microscopy. J. Biophys. Biochem. Cytol. **10:**475–503.
8. **Doms, R. W., R. Blumenthal, and B. Moss.** 1990. Fusion of intracellular and extracellular forms of vaccinia virus with the cell membrane. J. Virol. **64:** 4884–4892.
9. **Earl, P. L., and B. Moss.** 1991. Preparation of cell cultures and vaccinia virus stocks, p. 16.16.1–16.16.7. *In* F. M. Ausubel, R. Brent, R. E. Kingston, D. D. Moore, J. G. Seidman, J. A. Smith, and K. Struhl (ed.), Current protocols in molecular biology. Greene Publishing and Wiley Interscience, New York.
10. **Easterbrook, K. B.** 1966. Controlled degradation of vaccinia virions in vitro: an electron microscopic study. J. Ultrastruct. Res. **14:**484–496.
11. **Fenner, F., R. Wittek, and K. R. Dumbell.** 1989. The orthopoxviruses. Academic Press, San Diego, Calif.
12. **Griffiths, G.** 1993. Fine structure immunocytochemistry. Springer Verlag, Heidelberg, Germany.
13. **Grimley, P. M., E. N. Rosenblum, S. J. Mims, and B. Moss.** 1970. Interruption by rifampicin of an early stage in vaccinia virus morphogenesis: accumulation of membranes which are precursors of virus envelopes. J. Virol. **6:**519–533.
14. **Hiller, G., and K. Weber.** 1985. Golgi-derived membranes that contain an acylated viral polypeptide are used for vaccinia virus envelopment. J. Virol. **55:**651–659.
15. **Holowczak, J. A.** 1972. Uncoating of poxviruses. I. Detection and characterization of subviral particles in the uncoating process. Virology **50:**216–232.
16. **Holowczak, J. A., and W. K. Joklik.** 1967. Studies of the structural proteins of virions and cores. Virology **33:**717–725.
17. **Ichihashi, Y., M. Oie, and T. Tsuruhara.** 1984. Location of DNA-binding proteins and disulfide-linked proteins in vaccinia virus structural elements. J. Virol. **50:**929–938.
18. **Ichihashi, Y., T. Tsuruhara, and M. Oie.** 1983. The effect of proteolytic enzymes on the infectivity of vaccinia virus. Virology **122:**279–289.
19. **Joklik, W. K.** 1966. The poxviruses. Bacteriol. Rev. **30:**33–66.
20. **Joklik, W. K., and Y. Becker.** 1964. The replication and coating of vaccinia DNA. J. Mol. Biol. **10:**452–474.
21. **Kane, E. M., and S. Shuman.** 1993. Vaccinia virus morphogenesis is blocked by a temperature-sensitive mutation in the I7 gene that encodes a virion component. J. Virol. **67:**2689–2698.
22. **Krijnse Locker, J., M. Ericsson, P. Rottier, and G. Griffiths.** 1994. Characterization of the budding compartment of mouse hepatitis virus. J. Cell Biol. **124:**55–70.
23. **Krijnse Locker, J., J. K. Rose, M. C. Horzinek, and P. J. M. Rottier.** 1992. Membrane assembly of the triple-spanning coronavirus M protein. J. Biol. Chem. **267:**21911–21918.
24. **Morgan, C.** 1976. The insertion of DNA into vaccinia virus. Science **193:** 591–592.
25. **Moss, B.** 1990. Poxviridae and their replication, p. 2079–2103. *In* B. N. Fields, D. M. Knipe, R. M. Chanock, M. S. Hirsch, J. L. Melnick, T. P. Monath, and B. Roizman (ed.), Virology. Raven Press, New York.
26. **Moss, B., and E. N. Rosenblum.** 1973. Protein cleavage and poxvirus morphogenesis: tryptic peptide analysis of core precursors accumulated by blocking assembly with rifampicin. J. Mol. Biol. **81:**267–269.
27. **Moss, B., E. N. Rosenblum, E. Katz, and P. M. Grimley.** 1969. Rifampicin: a specific inhibitor of vaccinia virus assembly. Nature (London) **224:**1280–1284.
28. **Niles, E. G., and J. Seto.** 1988. Vaccinia virus gene D8 codes for a virion transmembrane protein. J. Virol. **62:**3772–3778.
29. **Payne, L. G.** 1978. Polypeptide composition of extracellular enveloped vaccinia virus. J. Virol. **27:**28–37.
30. **Rodriguez, D., J. R. Rodriguez, and M. Esteban.** 1992. Insertional inactivation of the vaccinia virus 32-kilodalton gene is associated with attenuation in mice and reduction of viral gene expression in polarized epithelial cells. J. Virol. **66:**183–189.
31. **Rodriguez, D., J.-R. Rodriguez, and M. Esteban.** 1993. The vaccinia virus 14-kilodalton fusion protein forms a stable complex with the processed protein encoded by the vaccinia virus A17L gene. J. Virol. **67:**3435–3440.
32. **Rodriguez, J. F., R. Janeczko, and M. Esteban.** 1985. Isolation and characterization of neutralizing monoclonal antibodies to vaccinia virus. J. Virol. **56:**482–488.
33. **Rodriguez, J. F., E. Paez, and M. Esteban.** 1987. A 14,000-M_r envelope protein of vaccinia virus is involved in cell fusion and forms covalently linked trimers. J. Virol. **61:**395–404.
34. **Rodriguez, J. F., and G. F. Smith.** 1990. IPTG-dependent vaccinia-virus: identification of a virus protein enabling virion envelopment by Golgi membranes and egress. Nucleic Acids Res. **18:**5347–5351.
35. **Rosel, J., and B. Moss.** 1985. Transcriptional and translational mapping and nucleotide sequence analysis of a vaccinia virus gene encoding the precursor of the major core polypeptide 4b. J. Virol. **56:**830–838.
36. **Sarov, I., and W. K. Joklik.** 1972. Isolation and characterization of intermediates in vaccinia virus morphogenesis. Virology **52:**223–233.
37. **Sarov, I., and W. K. Joklik.** 1972. Studies on the nature and location of the capsid polypeptides of vaccinia virions. Virology **50:**579–592.
38. **Sarov, I., and W. K. Joklik.** 1972. Characterization of intermediates in the uncoating of vaccinia virus DNA. Virology **50:**593–602.
39. **Schmelz, M., B. Sodeik, M. Ericsson, E. J. Wolffe, H. Shida, G. Hiller, and G. Griffiths.** 1994. Assembly of vaccinia virus: the second wrapping cisterna is derived from the trans Golgi network. J. Virol. **68:**130–147.
40. **Silver, M., and S. Dales.** 1982. Biogenesis of vaccinia: interrelationship between post-translational cleavage, virus assembly, and maturation. Virology **117:**341–356.

41. **Sodeik, B.** 1992. Das Assembly des Vaccinia Virus. Ph.D. thesis. European Molecular Biology Laboratory, Heidelberg, Germany.
42. **Sodeik, B., S. Cudmore, M. Ericsson, M. Esteban, E. G. Niles, and G. Griffiths.** 1995. Assembly of vaccinia virus: incorporation of p14 and p32 into the membrane of the intracellular mature virus. J. Virol. **69:**3560–3574.
43. **Sodeik, B., R. W. Doms, M. Ericsson, G. Hiller, C. E. Machamer, W. van't Hof, G. van Meer, B. Moss, and G. Griffiths.** 1993. Assembly of vaccinia virus: role of the intermediate compartment between the endoplasmic reticulum and the Golgi stacks. J. Cell Biol. **121:**521–541.
44. **Sodeik, B., G. Griffiths, M. Ericsson, B. Moss, and R. W. Doms.** 1994. Assembly of vaccinia virus: effects of rifampin on the intracellular distribution of viral protein p65. J. Virol. **68:**1103–1114.
45. **Tartaglia, J., A. Piccini, and E. Paoletti.** 1986. Vaccinia virus rifampicin-resistance locus specifies a late 63,000 Da gene product. Virology **150:**45–54.
46. **Van Meir, E., and R. Wittek.** 1988. Fine structure of the vaccinia virus gene encoding the precursor of the major core protein 4a. Arch. Virol. **102:**19–27.
47. **VanSlyke, J. K., C. A. Franke, and D. E. Hruby.** 1991. Proteolytic maturation of vaccinia virus core proteins: identification of a conserved motif at the N termini of the 4b and 25K virion proteins. J. Gen. Virol. **72:**411–416.
48. **VanSlyke, J. K., and D. E. Hruby.** 1994. Immunolocalization of vaccinia virus structural proteins during virion formation. Virology **198:**624–635.
49. **VanSlyke, J. K., S. S. Whitehead, E. M. Wilson, and D. E. Hruby.** 1991. The multistep proteolytic maturation pathway utilized by vaccinia virus P4a protein: a degenerate conserved cleavage motif within core proteins. Virology **183:**467–478.
50. **Weir, J. P., and B. Moss.** 1985. Use of a bacterial expression vector to identify the gene encoding a major core protein of vaccinia virus. J. Virol. **56:**534–540.
51. **Yang, W. P., and W. R. Bauer.** 1988. Purification and characterization of vaccinia virus structural protein VP8. Virology **167:**578–584.
52. **Yang, W. P., S. Y. Kao, and W. R. Bauer.** 1988. Biosynthesis and post-translational cleavage of vaccinia virus structural protein VP8. Virology **167:**585–590.